The effect of quantum fluctuations on the ferromagnetic-helix transition in a Heisenberg tetragonal lattice with competing in-plane interactions

1989 J. Phys.: Condens. Matter 1 3821

(http://iopscience.iop.org/0953-8984/1/24/005)

J. Phys.: Condens. Matter 1 (1989) 3821–3831. Printed in the UK

The effect of quantum fluctuations on the ferromagnetic–helix transition in a Heisenberg tetragonal lattice with competing in-plane interactions

A B Harris†, A Pimpinelli‡, E Rastelli‡ and A Tassi‡

† Department of Physics, University of Pennsylvania, Philadelphia, PA 19104, USA
‡ Dipartimento di Fisica dell'Universitá, 43100 Parma, Italy

Received 3 August 1988, in final form 3 January 1989

Abstract. Perturbative treatments of quantum fluctuations in Heisenberg helimagnets starting from the classical approximation fail because for $S \to \infty$ the spin wave is well defined only for a fixed helix wavevector $\boldsymbol{Q}$. Recently an exact T-matrix evaluation of the contribution to the ground-state energy from long-wavelength quantum fluctuations near the classical ferromagnet–helix (F-H) transition line was performed in order to discuss the zero-temperature phase diagram in the j_2–J_3 plane, where j_2 (j_3) sets the scale of second (third) neighbour interactions in the basal plane. For the hexagonal lattice it was shown that quantum fluctuations could change from second to first order the F-H transition near the F-AF-H classical triple point, where AF denotes antiferromagnet. Here we give analogous calculations on a tetragonal lattice, which show unexpected lattice-dependent features. In addition to a behaviour similar to that found on the hexagonal lattice near the F-AF-H triple point, the change of the order of transition is found also on a semi-infinite part of the classical F-H phase boundary.

1. Introduction

Only recently have people realised that no systematic perturbative approach exists to account for quantum corrections concerning Heisenberg helimagnets [1]. Troubles appear in evaluating quantum effects both for the phase diagram in parameter space and the spin-wave excitation energy spectrum, because in the classical approximation ($S \to \infty$) normal modes are well defined only for a particular value of the helix wavevector, $\boldsymbol{Q}_c$, so that also the zero-point motion energy is well defined only when the helix wavevector, $\boldsymbol{Q}$, actually is equal to $\boldsymbol{Q}_c$. Thus it is hard to assess directly the influence of quantum fluctuations on the true value of $\boldsymbol{Q}$. In particular, a perturbative expansion in $1/S$ leads to an imaginary magnon spectrum frequency in the neighbourhood of $\boldsymbol{Q}_c$. This indicates that the assumed ground state is not stable. A partial answer to the problem of quantum corrections to the classical phase diagram at $T = 0$ of a Heisenberg helimagnet was obtained by extrapolating the zero-point motion energy beyond the classical phase boundary [2].

A more controlled approach has been developed by Harris and Rastelli (HR) [3] to treat the neighbourhood of the ferromagnet–helix (F-H) phase boundary, where an expansion of the ground-state energy in powers of Q is realistic. In this case one can perform an exact T-matrix calculation [4] to all orders in $1/S$ within the small-Q expansion. This method has been applied to a hexagonal lattice within a model in

0953-8984/89/243821+11$02.50

which exchange interactions with second and third nearest-neighbouring spins in the basal plane compete with ferromagnetic nearest-neighbour interactions [3]. Thereby the F–H transition at zero temperature was predicted to be discontinuous near the F–AF–H triple point of the classical phase diagram at $T = 0$, where AF denotes antiferromagnet. In contrast, the first order in $1/S$ approach predicts a continous F–H transition, leaving the classical result unaltered [2].

In this paper we perform an analogous calculation for a simple tetragonal lattice with in-plane competing interactions up to third-nearest neighbours. In analogy with the results for the hexagonal lattice, we find that quantum fluctuations can cause the F–H transition to become discontinuous, especially when the spin is greater than 1/2. This discontinuous region appears for a large range of plausible values of the exchange integrals.

2. *T*-matrix treatment of quantum fluctuations

The Hamiltonian of our model reads

$$H = -\sum_{\alpha} J_{\alpha} \sum_{i,\delta_{\alpha}} \boldsymbol{S}_i \cdot \boldsymbol{S}_{i+\delta_{\alpha}} - J' \sum_{i,\delta'} \boldsymbol{S}_i \cdot \boldsymbol{S}_{i+\delta'} \tag{1}$$

where $\boldsymbol{\delta}_{\alpha}$ and $\boldsymbol{\delta}'$ are vectors joining site i with its neighbours of the αth shell and with its out-of-plane nearest neighbours NN, respectively. Here the $\widetilde{\text{NN}}$ in-plane J_1 and the out-of-plane J' exchange couplings are positive, while the next-nearest neighbours (NNN) J_2 and the third-nearest neighbours (TNN) J_3 coupling can have either sign. If J_2 and/or J_3 are negative, the competition between exchange interactions can lead to helical states. On the other hand, there is no competition due to J': the spins in each basal plane have identical orientations. The phase diagram at $T = 0$ in the classical approximation [5] is shown in figure 1. As one can see, two collinear phases F and AF and two H phases (H1 and H2) exist. H1 and H2 are characterised by helix wavevectors parallel to $\boldsymbol{\delta}_1$ and to $\boldsymbol{\delta}_2$, respectively.

Following HR we study the effect of quantum zero-point fluctuations in the vicinity of the F–H phase boundary. In such a calculation one writes the spin operators in terms of Bose creation and destruction operators by means of the Dyson–Maleev [6,7] transformation, in which the boson vacuum corresponds to a helix of wavevector $\boldsymbol{Q}$, with $aQ \ll 1$, where a is the in-plane lattice constant. Then one keeps only interaction potentials contributing to the T-matrix evaluation of the ground-state energy up to order Q^4.

Following this procedure, it is shown (HR) that the Hamiltonian (1) reduces to

$$\begin{aligned} H = E_0(\boldsymbol{Q}) + \sum_{k} A_k a_k^{\dagger} a_k + \frac{1}{2} \sum_{k} B_k (a_k^{\dagger} a_{-k}^{\dagger} + a_k a_{-k}) \\ + (2NS)^{-1} \sum_{1,2,3,4} V_{1,2,3,4} \delta(1+2,3+4) a_1^{\dagger} a_2^{\dagger} a_3 a_4 \end{aligned} \tag{2}$$

where 1 denotes $\boldsymbol{k}_1$, 2 denotes $\boldsymbol{k}_2$, etc and

$$\begin{aligned} E_0(\boldsymbol{Q}) = -4J_1 NS^2 [1 + j_2 + j_3 + j'/2 - \tfrac{1}{4}(aQ)^2(1 + 2j_2 + 4j_3) \\ + \tfrac{1}{48} a^4 (Q_x^4 + Q_y^4)(1 + 2j_2 + 16j_3) + \tfrac{1}{4} j_2 a^4 Q_x^2 Q_y^2] \end{aligned} \tag{3}$$

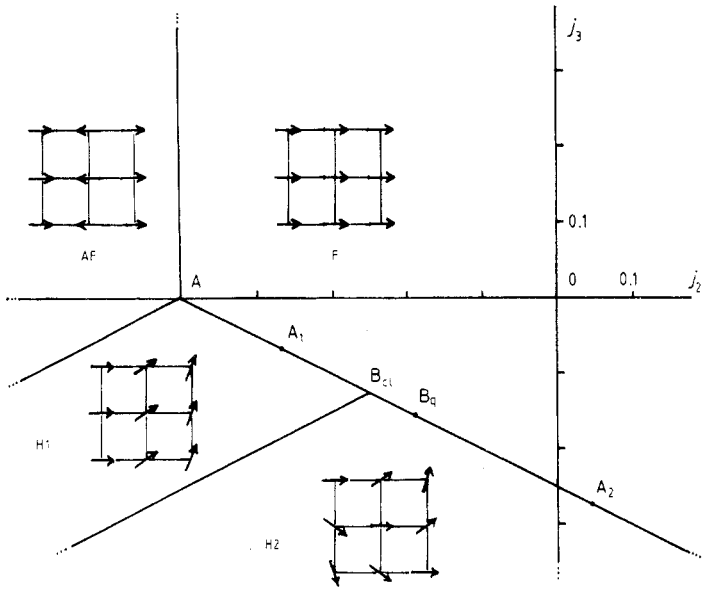

Figure 1. Zero-temperature phase diagram of the Heisenberg model on a tetragonal lattice showing the various phases, AF, F, H1, H2. The solid lines are phase boundaries for $S = \infty$, the classical model. For the quantum model for $j' = 0$ (no interplane coupling) we show for $S = 1/2$ the point B_q, the location of the H1 H2 F multicritical point, including quantum fluctuations, for $S = 1$ the point A_1, the limit of the regime B_q–A_1 over which the F H1 transition is continuous, and, for $S = 1/2$, A_2, the limit of the regime B_q–A_2 over which the F H2 transition is continuous. Outside the interval A_1–A_2 the F H transitions are discontinuous and occur inside the region of metastability of the F phase, as shown in figure 6 of [3].

with $j_\alpha = J_\alpha/J_1$, $j' = J'/J_1$, $A_k = 8J_1S\epsilon_k$, where

$$\epsilon_k = \frac{1}{2}\sum_{m=1}^{7} \hat{j}_m(1 - \cos k_m). \tag{4}$$

Here

$$\hat{j}_1 = \hat{j}_2 = 1 \qquad \hat{j}_3 = \hat{j}_4 = j_2 \qquad \hat{j}_5 = \hat{j}_6 = j_3 \qquad \hat{j}_7 = j' \tag{5}$$

and

$$\begin{aligned} &k_1 = ak_y \qquad k_2 = ak_x \qquad k_3 = a(k_x + k_y) \qquad k_4 = a(k_x - k_y) \\ &k_5 = 2ak_y \qquad k_6 = 2ak_x \qquad k_7 = ck_z \end{aligned} \tag{6}$$

where c is the out-of-plane lattice constant. Also in equation (2)

$$B_k = -8J_1S[\tfrac{1}{4}b_k^{(1)}(aQ_x)^2 + \tfrac{1}{4}b_k^{(2)}(aQ_y)^2 + \tfrac{1}{2}\eta_k a^2 Q_x Q_y] \tag{7}$$

where

$$b_k^{(1)} = \tfrac{1}{2}[\cos k_1 + j_2(\cos k_3 + \cos k_4) + 4j_3 \cos k_5] \tag{8}$$

$$b_k^{(2)} = \tfrac{1}{2}[\cos k_2 + j_2(\cos k_3 + \cos k_4) + 4j_3 \cos k_6] \tag{9}$$

$$\eta_k = \tfrac{1}{2} j_2(\cos k_3 - \cos k_4) \tag{10}$$

and $V_{1,2,3,4}$ is the well known Dyson–Maleev [6,7] interaction potential, whose form (HR) is only needed for the special case $\boldsymbol{k}_1 = -\boldsymbol{k}_2 \equiv \boldsymbol{k}$, and $\boldsymbol{k}_3 = -\boldsymbol{k}_4 \equiv \boldsymbol{q}$, and $V_{1,2,3,4}$ for these values of momenta, denoted $V_{\boldsymbol{k},\boldsymbol{q}}$, is given as

$$V_{\boldsymbol{k},\boldsymbol{q}} = -4J_1 S \sum_{m=1}^{7} \hat{\jmath}_m (1 - \cos k_m)(1 - \cos q_m). \tag{11}$$

The exact ground-state energy obtained by the T-matrix calculation within Q^4 contributions reads [3]

$$E_G(\boldsymbol{Q}) = E_0(\boldsymbol{Q}) - (1/4) \sum_{\boldsymbol{k}} B_{\boldsymbol{k}}^2 / A_{\boldsymbol{k}} + (1/8NS) \sum_{\boldsymbol{k},\boldsymbol{q}} B_{\boldsymbol{k}} B_{\boldsymbol{q}} T_{\boldsymbol{k},\boldsymbol{q}} / (A_{\boldsymbol{k}} A_{\boldsymbol{q}}) \tag{12}$$

where $T_{\boldsymbol{k},\boldsymbol{q}}$ is the solution of

$$T_{\boldsymbol{k},\boldsymbol{q}} = V_{\boldsymbol{k},\boldsymbol{q}} - (1/2NS) \sum_{\boldsymbol{p}} V_{\boldsymbol{k},\boldsymbol{p}} T_{\boldsymbol{p},\boldsymbol{q}} / A_{\boldsymbol{p}} \tag{13}$$

which we write in the form

$$T_{\boldsymbol{k},\boldsymbol{q}} = -4J_1 S \sum_{m,n=1}^{7} \hat{\jmath}_m (\mathbf{A}^{-1})_{m,n} (1 - \cos k_m)(1 - \cos q_n) \tag{14}$$

where the matrix $\mathbf{A}$ is defined as

$$A_{m,n} = \delta_{m,n} - \hat{\jmath}_n D_{m,n} / (2S) \tag{15}$$

with

$$D_{m,n} = D_{n,m} = (1/2N) \sum_{\boldsymbol{k}} (1 - \cos k_m)(1 - \cos k_n) / \epsilon_{\boldsymbol{k}}. \tag{16}$$

For the tetragonal lattice these sums over the three-dimensional Brillouin zone can be reduced to two-dimensional integrals. Expressions for the $D_{m,n}$ and the sum rules they obey are given in the Appendix. There we also obtain the following expression for the reduced ground-state energy, $e_G(\boldsymbol{Q}) \equiv E_G(\boldsymbol{Q})/(4J_1 S^2 N)$:

$$e_G(\boldsymbol{Q}) = e_0 + e_2 (aQ)^2 + (e_4^{(0)} + e_4^{(1)} \cos 4\theta)(aQ)^4 \tag{17}$$

where θ is the angle between $\boldsymbol{Q}$ and $\boldsymbol{\delta}_1$ and

$$e_0 = -(1 + j_2 + j_3 + j'/2) \tag{18}$$

$$e_2 = (1 + 2j_2 + 4j_3)/4 \tag{19}$$

$$e_4^{(0)} = -(1 + 4j_2 + 16j_3)/64 - [3I_0 + I_0' - (3I_1 + I_1')/(2S)]/(128S) \tag{20}$$

$$e_4^{(1)} = -(1 - 4j_2 + 16j_3)/192 - [I_0 - I_0' - (I_1 - I_1')/(2S)]/(128S) \tag{21}$$

where I_0, I_0', I_1 and I_1' are integrals given in equations (A17)–(A21) of the Appendix.

We now discuss the significance of equation (17). First of all, the F–H phase boundary is defined by the vanishing of e_2, i.e. it is given by

$$1 + 2j_2 + 4j_3 = 0. \tag{22}$$

As for the hexagonal lattice, e_2 has no quantum corrections. On the F–H phase boundary the term proportional to Q^2 is missing and the ground-state energy reduces to

$$e_G(\mathrm{H1}) = e_0 + (e_4^{(0)} + e_4^{(1)} \cos 4\theta) a^4 Q^4 \tag{23}$$

so that one obtains a helix of type H1 ($\theta = 0$) for $e_4^{(1)} > 0$, and that of type H2 ($\theta = \pi/4$) for $e_4^{(1)} < 0$. We note that the H1–H2–F multicritical point is given by $e_4^{(1)} = 0$ and is shifted by quantum corrections from its classical position B_{cl} to the shifted point B_q, as shown in figure 1 for $S = 1/2$ and $j' = 0$. Here and in the following we consider the value $j' = 0$, even if long-range order (LRO) is lost in the 2D case, because it is illustrative of the behaviour at very small interplane coupling. In table 1 we give the values of j_3 corresponding to point B_q, for representative values of S and j'. Note that the location of point B_q is only slightly dependent on j', whereas it is a more sensitive function of S. Notice that the shift from B_{cl} to B_q found by the T-matrix calculation amends the previous result obtained by a first order in $1/S$ approach where point B_{cl} remained unshifted [2]. In a separate paper [8] we study in greater detail the nature of the H1–H2 transition.

Table 1. Values of j_3 for which $e_4^{(1)} = 0$ and $e_2 = 0$ (which locates the H1–H2–F multicritical point) for selected values of S and j'. The corresponding values of j_2 are given by equation (22).

j'	$S = 1/2$	$S = 1$	$S = 5/2$
0	−0.1550	−0.1375	−0.1288
0.1	−0.1520	−0.1350	−0.1288
1	−0.1412	−0.1323	−0.1277

On the F–H phase boundary the ground-state energy, when minimised with respect to θ, will be

$$e_0 + (e_4^{(0)} - |e_4^{(1)}|)(aQ)^4 \equiv e_0 + e_{4t}(aQ)^4 \tag{24}$$

in which case one sees that the F–H transition will be discontinuous if e_{4t} is negative.

In the classical approximation $e_{4t} \geq 0$ over the whole F–H1 phase boundary. However, when quantum fluctuations are included, we find that e_{4t} is positive only over a restricted region of the F–H1 phase boundary. In table 2 we give the values of j_3 for which $e_{4t} = 0$ as function of S and j' on the F–H1 phase boundary.

In figure 1 point A_1 corresponds to $e_{4t} = 0$ in the quantum limit $S = 1$, $j' = 0$. In the region between points A_1 and the F–AF–H triple point a *quantum helix* (i.e. a helix stabilised by quantum fluctuations) of the type H1 should be stable so that a first-order F–H transition line may occur in this region, as we discuss below. The fact is analogous

Table 2. Values of j_3 for which $e_{4t} = 0$ on the F–H1 phase boundary for selected values of S and j'. The corresponding values of j_2 are given by equation (22).

j'	$S = 1/2$	$S = 1$	$S = 5/2$
0	−0.1184	−0.0673	−0.0373
0.1	−0.0893	−0.0524	−0.0279
1	−0.0545	−0.0319	−0.0159

to what happens on the hexagonal lattice, but on the tetragonal lattice the same occurs for helix H2 far from the triple point A.

In table 3 we give the values of j_3 at which e_{4t}, the coefficient of Q^4 in equation (24), becomes negative on the F–H2 phase boundary. In figure 1 point A_2 corresponds to $S = 1/2$, $j' = 0$. Notice that the Hamiltonian parameters involved have plausible magnitudes. The F–H2 phase transition is discontinuous in the interval where e_{4t} is negative.

Table 3. Values of j_3 for which $e_{4t} = 0$ on the F–H2 phase boundary for selected values of S and j'. The corresponding values of j_2 are given by equation (22).

j'	$S = 1/2$	$S = 1$	$S = 5/2$
0	−0.2723	−0.4366	−0.7317
0.1	−0.3834	−0.5558	−0.9053
1	−0.5275	−0.7493	−1.2150

The reason for the sign change of the Q^4 coefficient near the triple point A and in the semi-infinite part of the F–H classical phase boundary from point A_2, is the softness of the spin waves along the F–H transition line for $j_3 \to 0$ (A) and $j_3 \to -\infty$. It is instructive to explicitly display the modes corresponding to these soft lines. Consider first the situation near the triple point A, where $J_2 = -(1/2)J_1$. It is easy to verify that it costs no energy, starting from the antiferromagnetic structure to rotate each column of spins in figure 1 through an arbitrary angle θ_i, where i labels the column, as shown in figure 2(*a*). This degree of freedom clearly corresponds to having zero-energy spin waves along the axis, $k_y = 0$ where the y axis is along the direction of the columnar axis. A similar construction, shown in figure 2(*b*), shows that it also costs no energy, starting from the antiferromagnetic structure, to rotate each row of spins through an arbitrary angle θ_j, where j labels the row. This degeneracy indicates that spin waves having $k_x = 0$ have zero energy. In both cases the cost in energy is zero because the exchange field from two nearest neighbours is exactly balanced by that from four next-nearest neighbours. The discussion for the case $j_3 \to -\infty$ on the F–H phase boundary is very similar and is illustrated in figure 2(*c*) and 2(*d*). There one has that J_1 is negligible and $J_3 = -(1/2)J_2$. But for these parameters the model can be considered to be two independent interpenetrating square lattices in which J_3 and J_2 play the roles previously played at point A by J_2 and J_1. Because the square lattices here are rotated by 45°, one has zero-energy spin waves over the lines $k_x = \pm k_y$.

The picture given above indicates that the F–H transition remains second order only for a finite interval (A_1A_2) of the infinite boundary line. A question arises whether or not this finite interval reaches the *new* triple point A′ shifted by quantum effects. In order to assess the reliability of the long-wavelength quantum helix near the F–AF–H

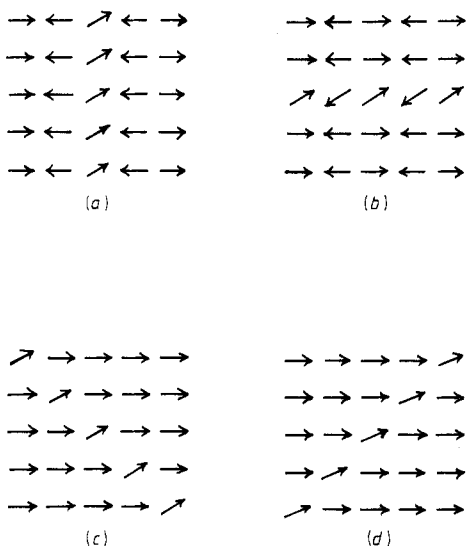

Figure 2. Zero-energy modes at the triple point F–AF–H1 are shown in (*a*) and (*b*). The spins of any NN column (*a*) or row (*b*) can rotate freely of an arbitrary angle with respect to the antiferromagnetic background. Zero-energy modes along the F–H transition line for $j_3 \to -\infty$ are shown in (*c*) and (*d*). The spins of any NNN line can rotate freely of an arbitrary angle with respect to the ferromagnetic background.

triple point, we evaluate quantum corrections to the AF ground state at leading order in $1/S$, since in the AF configuration it is impossible to perform calculations to all orders in $1/S$ as for the helix with small-$\boldsymbol{Q}$ wavevectors. It is well known that quantum corrections shift the AF–F transition line towards the ferromagnetic region [2]. In order to estimate this shift we evaluate the ground-state energy of the antiferromagnetic phase in the ferromagnetic region, evaluating then the first-order quantum correction along the classical AF–F boundary. Figures 3(*a–c*) show the new AF–F transition lines for selected values of S for $j' = 0$, $j' = 0.1$ and $j' = 1$, respectively. The points along the F–H transition lines are obtained from the T-matrix calculations truncated at the leading order in $1/S$. Their location is practically unchanged with respect to a T-matrix evaluation to all orders in $1/S$ (see table 1). These results seem to indicate that the AF phase should be able to prevent the occurence of the quantum helix only for $S = 1/2$ for any interplane exchange coupling J'.

For any $S \geq 1$ the existence of the quantum helix should be assured, independent of the value of j'. In any case the quantum helix extends over a narrow range in the neighbourhood of the new triple point A′ whose exact location is at present an open question. On the contrary, a semi-infinite region exists where a quantum helix of the H2 kind is stable. This is a striking new result with respect to the hexagonal lattice, on which the existence of a H2 helix was prevented by the presence of a 120°-phase [3].

An interesting question arises about the kind of phase one has at finite temperature along the F–H transition line. It is easy to see that the order parameter

$$\langle S_i^z \rangle = S - (1/N) \sum_{\boldsymbol{k}} \langle a_{\boldsymbol{k}}^+ a_{\boldsymbol{k}} \rangle \tag{25}$$

where S_i^z is the component of the spin along the local quantisation axis, diverges on the

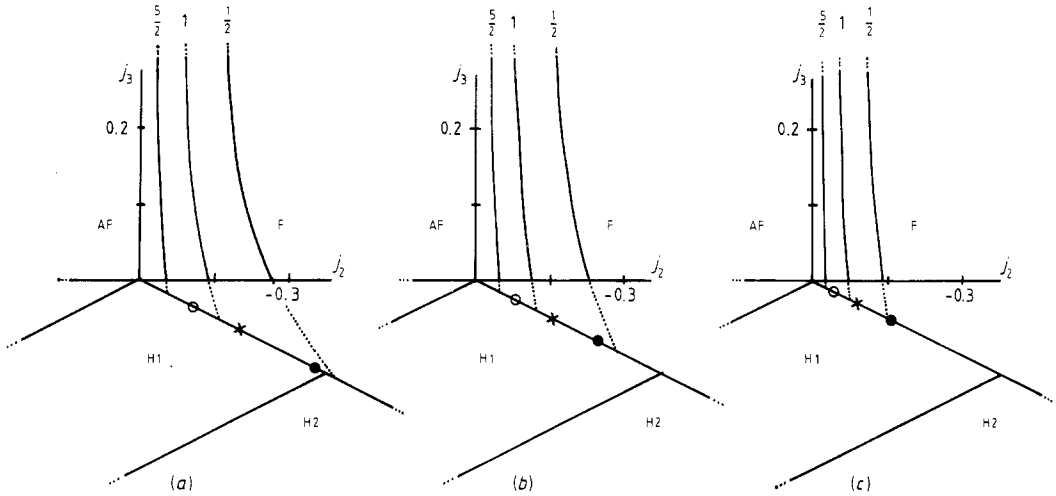

Figure 3. Phase diagrams for various values of j' ($j' = 0$ in (*a*), $j' = 0.1$ in (*b*) and $j' = 1$ in (*c*)) and S (the values of S, 5/2, 1, and 1/2, are indicated at the top of each curve) which show the relative locations of point A_1, the limit of continuous F–H1 transitions, here indicated by an open circle for $S = 5/2$, a cross for $S = 1$, and a full circle for $S = 1/2$, and the extrapolated (shown by dotted curves) limit of the F–AF phase boundary as calculated to lowest order in a $1/S$ expansion. For a given spin value, if the extrapolated limit lies outside the interval B_q–A_1, there will be a regime of discontinuous F–H1 phase transitions as shown in figure 6 of [3]. Otherwise, the F–H1 transition is always continuous.

whole interval A_1A_2 because the spin-wave spectrum behaves for small $\boldsymbol{k}$ wavevectors like

$$E_{\boldsymbol{k}} \simeq 2J_1S[-j_3a^4(k_x^4 + k_y^4) + (1/2)(1 + 4j_3)a^4k_x^2k_y^2 + j'(ck_z)^2] \tag{26}$$

so that no LRO is expected at any finite temperature for three-dimensional ($j' > 0$) systems. Here we do not take the 2D-case into account because for $j' = 0$, LRO is lost at any finite temperature in the whole parameter space, whereas we are interested, in particular, in the peculiarities of the F–H transition line. Anyway, the divergence in equation (25) is logarithmic as for a 2D Heisenberg or XY ferromagnet. We recall here that in a classical 2D Heisenberg ferromagnet the disordered phase is a paramagnetic one, whereas in a classical 2D XY ferromagnet it is a Kosterlitz–Thouless [9] phase, characterised by an algebraic decay of the correlation function. It is worth noticing that this unorthodox phase is prevented in the 2D Heisenberg model because of the presence of unbound vortices which, on the contrary, have a divergent cost in energy in the XY model.

Moreover it has been shown [10] that the XY version of the Hamiltonian (1), treated in the classical ($S \to \infty$) harmonic approximation, exhibits a Kosterlitz–Thouless low-temperature phase on the F–H transition line. The same result has been obtained rigorously by Amit and co-workers [11] at the H1–H2–F triple point B_{cl}. We also notice that for the Heisenberg model the same algebraic decay of the correlation function is obtained in the spin-wave approximation on the F–H line. We believe that this indication could be realistic because there is no evidence of the existence of unbound vortex-like excitations in 3D systems. On the other hand Kawamura found that the classical antiferromagnetic Heisenberg model on both the triangular and the

hexagonal [12] lattice seems to show the same critical behaviour as the corresponding classical XY antiferromagnet. This is in contrast with what happens in 2D for collinear configurations.

3. Summary and conclusions

In this paper we have studied the effects of long-wavelength quantum fluctuations on the ground-state energy of a tetragonal Heisenberg model with in-plane competing interactions up to third-nearest neighbours, in the neighbourhood of the F–H transition line. The approach we use is a T-matrix calculation exact within Q^4 contributions as it has already been performed for the corresponding hexagonal model [3].

The main result we find is a change from second to first order of the F–H phase transition. This occurs in the neighbourhood of the F–AF–H triple point, owing to quantum fluctuations, as it happens on the hexagonal lattice [3]. However, the tetragonal helimagnet shows an unexpected quantum helix phase on a semi-infinite part of the classical F–H phase boundary in the phase space of competing exchange interactions shown in figure 1. On the hexagonal lattice this phase was prevented by the presence of the 120°-three sublattice phase. We stress that this region includes plausible values of the exchange interactions.

Appendix

Here we record explicit expressions for the $D_{m,n}$.

$$D_{11} = (2\pi^2)^{-1} \int_0^\pi \int_0^\pi \mathrm{d}x\,\mathrm{d}y\,(1-\cos y)^2/D(x,y) \tag{A1}$$

$$D_{12} = (2\pi^2)^{-1} \int_0^\pi \int_0^\pi \mathrm{d}x\,\mathrm{d}y\,(1-\cos y)(1-\cos x)/D(x,y) \tag{A2}$$

$$D_{13} = (2\pi^2)^{-1} \int_0^\pi \int_0^\pi \mathrm{d}x\,\mathrm{d}y\,(1-\cos y)(1-\cos x\cos y)/D(x,y) \tag{A3}$$

$$D_{15} = (2\pi^2)^{-1} \int_0^\pi \int_0^\pi \mathrm{d}x\,\mathrm{d}y\,(1-\cos y)(1-\cos 2y)/D(x,y) \tag{A4}$$

$$D_{16} = (2\pi^2)^{-1} \int_0^\pi \int_0^\pi \mathrm{d}x\,\mathrm{d}y\,(1-\cos y)(1-\cos 2x)/D(x,y) \tag{A5}$$

$$D_{33} = (2\pi^2)^{-1} \int_0^\pi \int_0^\pi \mathrm{d}x\,\mathrm{d}y\,[(1-\cos x\cos y)^2 + (\sin x\sin y)^2]/D(x,y) \tag{A6}$$

$$D_{34} = (2\pi^2)^{-1} \int_0^\pi \int_0^\pi \mathrm{d}x\,\mathrm{d}y\,[(1-\cos x\cos y)^2 - (\sin x\sin y)^2]/D(x,y) \tag{A7}$$

$$D_{35} = (2\pi^2)^{-1} \int_0^\pi \int_0^\pi \mathrm{d}x\,\mathrm{d}y\,(1-\cos 2y)(1-\cos x\cos y)/D(x,y) \tag{A8}$$

$$D_{55} = (2\pi^2)^{-1} \int_0^\pi \int_0^\pi \mathrm{d}x\,\mathrm{d}y\,(1-\cos 2y)^2/D(x,y) \tag{A9}$$

$$D_{56} = (2\pi^2)^{-1} \int_0^\pi \int_0^\pi \mathrm{d}x\,\mathrm{d}y\,(1-\cos 2x)(1-\cos 2y)/D(x,y) \tag{A10}$$

where

$$D(x,y) = \{\epsilon(x,y)[\epsilon(x,y)+j']\}^{1/2} \tag{A11}$$

$$\epsilon(x,y) = 1-(1/2)(\cos x+\cos y)+j_2(1-\cos x\cos y)+j_3[1-(1/2)(\cos 2x+\cos 2y)]. \tag{A12}$$

For symmetry reasons one has

$$\begin{aligned} &D_{22}=D_{11} \qquad D_{23}=D_{14}=D_{24}=D_{13} \qquad D_{26}=D_{15} \qquad D_{25}=D_{16} \\ &D_{44}=D_{33} \qquad D_{66}=D_{55} \qquad D_{36}=D_{45}=D_{46}=D_{35}. \end{aligned} \tag{A13}$$

The following sum rules hold.

$$D_{11}+D_{12}+2j_2D_{13}+j_3(D_{15}+D_{16})+j'D_{17}=1 \tag{A14}$$

$$2D_{13}+j_2(D_{33}+D_{34})+2j_3D_{35}+j'D_{37}=1 \tag{A15}$$

$$D_{15}+D_{16}+2j_2D_{35}+j_3(D_{55}+D_{56})+j'D_{57}=1 \tag{A16}$$

$$2D_{17}+2j_2D_{37}+2j_3D_{57}+j'D_{77}=1. \tag{A17}$$

Thus the D_{m7} ($m=1,\ldots,7$) are obtained from equations (A14)–(A17) through equations (A1)–(A10). Equation (12) then becomes

$$E_{\mathrm{G}}(\boldsymbol{Q}) = E_0(\boldsymbol{Q}) - 4J_1SN\{a^4(Q_x^4+Q_y^4)[I_0-I_1/(2S)]/32 + a^4Q_x^2Q_y^2[I_0'-I_1'/(2S)]/16\} \tag{A18}$$

where

$$I_0 = (4\pi^2)^{-1} \int_0^\pi \int_0^\pi \mathrm{d}x\,\mathrm{d}y\, b_1^2(x,y)/D(x,y) \tag{A19}$$

$$I_0' = (4\pi^2)^{-1} \int_0^\pi \int_0^\pi \mathrm{d}x\,\mathrm{d}y\,[b_1(x,y)b_1(y,x)-8(j_2\sin x\sin y)^2]/D(x,y) \tag{A20}$$

$$I_1 = -(1/2)\sum_{m,n=1}^{7} \hat{\jmath}_m(\mathbf{A}^{-1})_{mn}I_m^{(1)}I_n^{(1)} \tag{A21}$$

$$I_1' = -(1/2)\sum_{m,n=1}^{7} \hat{j}_m(\mathbf{A}^{-1})_{mn}[(1/2)(I_m^{(1)}I_n^{(2)} + I_m^{(2)}I_n^{(1)}) + 2I_m^{\eta}I_n^{\eta}] \tag{A22}$$

with

$$b_1(x, y) = \cos y + j_2 \cos x \cos y + 4j_3 \cos 2y \tag{A23}$$

$$I_m^{(i)} = (1/N)\sum_k b_k^{(i)}(1 - \cos k_m)/\epsilon_k \qquad i = 1, 2 \tag{A24}$$

$$I_m^{\eta} = (1/N)\sum_k \eta_k(1 - \cos k_m)/\epsilon_k. \tag{A25}$$

The explicit expressions of $I_m^{(1)}$ and I_m^{η} for the tetragonal lattice read

$$I_1^{(1)} = (4\pi^2)^{-1}\int_0^{\pi}\int_0^{\pi} dx\,dy\, b_1(x, y)(1 - \cos y)/D(x, y) \tag{A26}$$

$$I_2^{(1)} = (4\pi^2)^{-1}\int_0^{\pi}\int_0^{\pi} dx\,dy\, b_1(x, y)(1 - \cos x)/D(x, y) \tag{A27}$$

$$I_3^{(1)} = I_4^{(1)} = (4\pi^2)^{-1}\int_0^{\pi}\int_0^{\pi} dx\,dy\, b_1(x, y)(1 - \cos x \cos y)/D(x, y) \tag{A28}$$

$$I_5^{(1)} = (4\pi^2)^{-1}\int_0^{\pi}\int_0^{\pi} dx\,dy\, b_1(x, y)(1 - \cos 2y)/D(x, y) \tag{A29}$$

$$I_6^{(1)} = (4\pi^2)^{-1}\int_0^{\pi}\int_0^{\pi} dx\,dy\, b_1(x, y)(1 - \cos 2x)/D(x, y) \tag{A30}$$

$$I_1^{(2)} = I_2^{(1)} \qquad I_2^{(2)} = I_1^{(1)} \qquad I_3^{(2)} = I_4^{(2)} = I_3^{(1)} \qquad I_5^{(2)} = I_6^{(1)} \qquad I_6^{(2)} = I_5^{(1)} \tag{A31}$$

$$I_1^{\eta} = I_2^{\eta} = I_5^{\eta} = I_6^{\eta} = 0 \tag{A32}$$

$$I_3^{\eta} = -I_4^{\eta} = -(j_2/\pi^2)\int_0^{\pi}\int_0^{\pi} dx\,dy\,(\sin x \sin y)^2/D(x, y) \tag{A33}$$

$$I_1^{(1)} + I_2^{(1)} + 2j_2I_3^{(1)} + j_3(I_5^{(1)} + I_6^{(1)}) + j'I_7^{(1)} = 0. \tag{A34}$$

Using these formulae one obtains equation (17) of the text.

References

[1] Rastelli E and Tassi A 1986 *J. Phys. C: Solid State Phys.* **19** 1993
[2] Rastelli E, Reatto L and Tassi A 1986 *J. Phys. C: Solid State Phys.* **19** 6623
[3] Harris A B and Rastelli E 1988 *J. Appl. Phys.* **63** 3083; 1989 *Phys. Rev.* B at press
[4] Silberglitt R and Harris A B 1967 *Phys. Rev. Lett.* **19** 30
[5] Rastelli E, Tassi A and Reatto L 1979 *Physica* B **97** 1
[6] Dyson F J 1986 *Phys. Rev.* **102** 1217
[7] Maleev S V 1958 *Sov. Phys.–JETP* **6** 776
[8] Harris A B, Rastelli E and Tassi A 1989 to be published
[9] Kosterlitz J M and Thouless D J 1973 *J. Phys. C: Solid State Phys.* **6** 1181
[10] Kaplan T A 1980 *Phys. Rev. Lett.* **44** 760
[11] Amit D J, Elitzur S, Rabinovici E and Savit R 1982 *Nucl. Phys.* B **210** 69
[12] Kawamura H 1987 *J. Appl. Phys.* **61** 3590